










# Multidirectional wall shear stress promotes advanced coronary plaque development: comparing five shear stress metrics

Ayla Hoogendoorn <sup>1</sup>, Annette M. Kok<sup>1</sup>, Eline M.J. Hartman<sup>1</sup>, Giuseppe de Nisco <sup>2</sup>, Lorena Casadonte <sup>3</sup>, Claudio Chiastra <sup>2</sup>, Adriaan Coenen<sup>1,4</sup>, Suze-Anne Korteland <sup>1</sup>, Kim Van der Heiden <sup>1</sup>, Frank J.H. Gijsen<sup>1</sup>, Dirk J. Duncker <sup>5</sup>, Antonius F.W. van der Steen <sup>1</sup>, and Jolanda J. Wentzel <sup>1\*</sup>

<sup>1</sup>Department of Cardiology, Biomedical Engineering, Erasmus MC, Dr. Molewaterplein 40, 3015 GD Rotterdam, The Netherlands; <sup>2</sup>PoliTo<sup>BIOMed</sup> Lab, Department of Mechanical and Aerospace Engineering, Politecnico di Torino, Turin, Italy; <sup>3</sup>Department of Biomedical Engineering and Physics, Amsterdam UMC, Amsterdam, The Netherlands; <sup>4</sup>Department of Radiology, Erasmus MC, Rotterdam, The Netherlands; and <sup>5</sup>Department of Cardiology, Experimental Cardiology, Erasmus MC, Rotterdam, The Netherlands

Received 23 May 2019; revised 15 July 2019; editorial decision 7 August 2019; accepted 20 August 2019; online publish-ahead-of-print 22 August 2019

**Time for primary review: 41 days**

## Aims

Atherosclerotic plaque development has been associated with wall shear stress (WSS). However, the multidirectionality of blood flow, and thus of WSS, is rarely taken into account. The purpose of this study was to comprehensively compare five metrics that describe (multidirectional) WSS behaviour and assess how WSS multidirectionality affects coronary plaque initiation and progression.

## Methods and results

Adult familial hypercholesterolaemic pigs ( $n=10$ ) that were fed a high-fat diet, underwent imaging of the three main coronary arteries at three-time points [3 ( $T_1$ ), 9 ( $T_2$ ), and 10–12 ( $T_3$ ) months]. Three-dimensional geometry of the arterial lumen, in combination with local flow velocity measurements, was used to calculate WSS at  $T_1$  and  $T_2$ . For analysis, arteries were divided into 3 mm/45° sectors ( $n=3648$ ). Changes in wall thickness and final plaque composition were assessed with near-infrared spectroscopy–intravascular ultrasound, optical coherence tomography imaging, and histology. Both in pigs with advanced and mild disease, the highest plaque progression rate was exclusively found at low time-averaged WSS (TAWSS) or high multidirectional WSS regions at both  $T_1$  and  $T_2$ . However, the eventually largest plaque growth was located in regions with initial low TAWSS or high multidirectional WSS that, over time, became exposed to high TAWSS or low multidirectional WSS at  $T_2$ . Besides plaque size, also the presence of vulnerable plaque components at the last time point was related to low and multidirectional WSS. Almost all WSS metrics had good predictive values for the development of plaque (47–50%) and advanced fibrous cap atheroma (FCA) development (59–61%).

## Conclusion

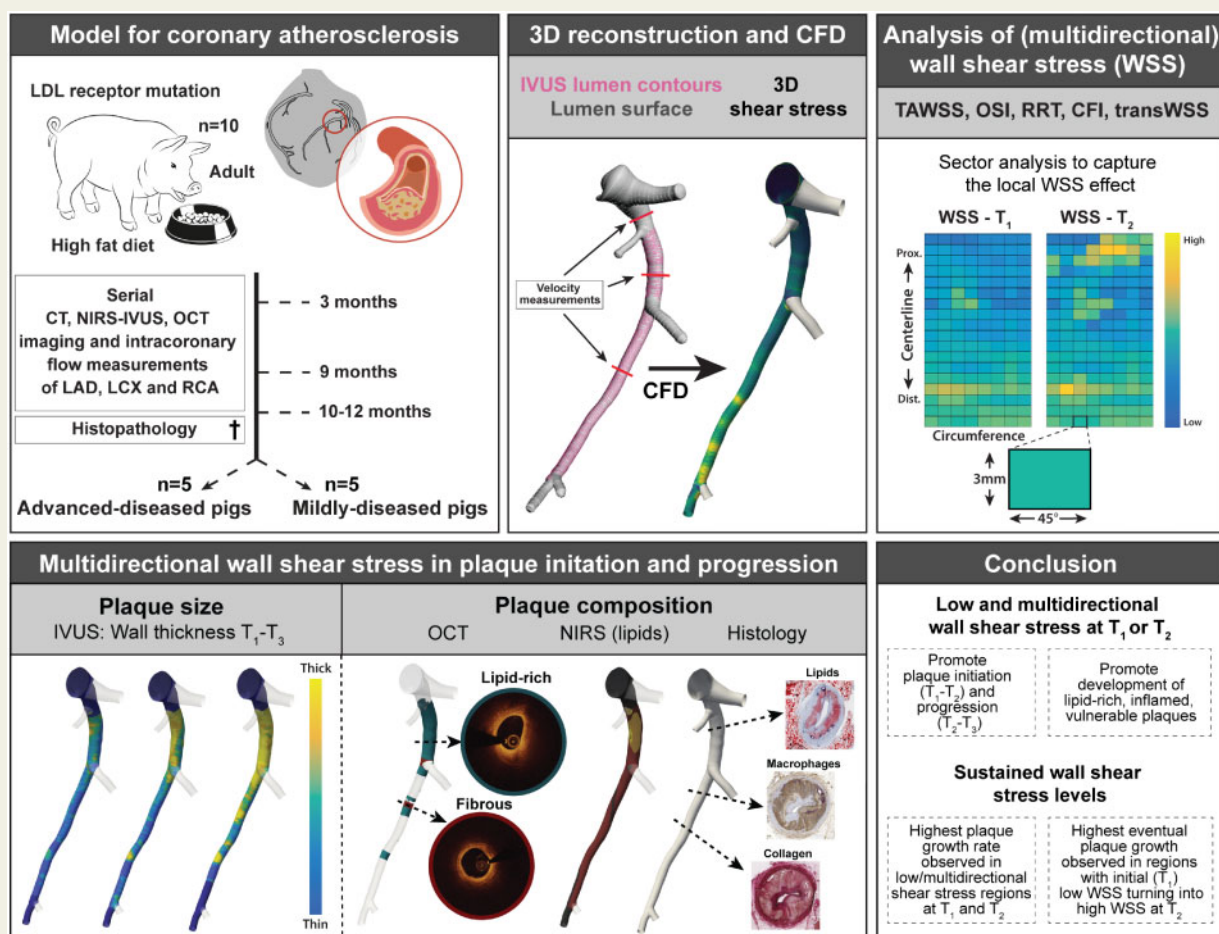
This study demonstrates that low and multidirectional WSS promote both initiation and progression of coronary atherosclerotic plaques. The high-predictive values of the multidirectional WSS metrics for FCA development indicate their potential as an additional clinical marker for the vulnerable disease.

\* Corresponding author. Tel: +31 10 7044 044; fax: +31 10 7044 720, E-mail: j.wentzel@erasmusmc.nl

© The Author(s) 2019. Published by Oxford University Press on behalf of the European Society of Cardiology.

This is an Open Access article distributed under the terms of the Creative Commons Attribution Non-Commercial License (<http://creativecommons.org/licenses/by-nc/4.0/>), which permits non-commercial re-use, distribution, and reproduction in any medium, provided the original work is properly cited. For commercial re-use, please contact [journals.permissions@oup.com](mailto:journals.permissions@oup.com)

## Graphical Abstract



## Keywords

Coronary artery disease • Atherosclerosis • Wall shear stress • Invasive imaging • Histopathology

## 1. Introduction

Ischaemic coronary artery disease (CAD), caused by destabilization and subsequent rupture of atherosclerotic plaques, is predicted to remain the leading cause of death.<sup>1</sup> Although the complex process of plaque development is incompletely understood, wall shear stress (WSS) is known to play a key role. WSS is a biomechanical metric that describes the frictional force between blood flow and the endothelial cells covering the arterial wall. Both pre-clinical and clinical studies showed an intricate role of WSS in (advanced) plaque development since both low and high WSS have been associated with plaque growth and destabilization.<sup>2-9</sup> To further elucidate the role of WSS in coronary atherosclerosis, longitudinal imaging studies are crucial. Moreover, since most studies only use time-averaged WSS (TAWSS) as a descriptor of disturbed blood flow, the multidirectionality of blood flow, induced by its pulsatile nature in combination with the three-dimensional geometry, is not taken into account. Therefore, in recent years, new WSS metrics have been developed to capture this multidirectional flow behaviour: the oscillatory shear index (OSI), relative residence time (RRT), transverse WSS (transWSS), and its normalized version: the cross-flow index (CFI)

(Table 1). The role of TAWSS, RRT, and OSI was demonstrated in a number of studies.<sup>9,12,13,15-17</sup> However, transWSS and CFI have not been investigated before in a longitudinal imaging study with histopathology. Since patient studies do not allow for multiple invasive imaging procedures and the collection of coronary tissue, we employed a highly relevant porcine model of familial hypercholesterolaemia<sup>18</sup> to study the effect of multidirectional WSS on plaque development. By using adult, full-grown pigs, we excluded the influence of growth-related changes in the geometry of the coronaries, important for serial assessment of WSS and plaque size. Serial, multimodality invasive imaging, combined with a detailed histological analysis enabled us to comprehensively compare five different (multidirectional) WSS metrics to assess how multidirectional WSS affects both plaque initiation and progression.

## 2. Methods

A detailed description of the surgery protocol, anaesthesia and euthanasia, blood and tissue processing, computational modelling and of the histology, imaging, and WSS analysis is provided in the [Supplementary](#)

**Table 1** Overview of the (multidirectional) shear stress metrics

Shear stress metric	Description	References
Time-averaged wall shear stress (TAWSS)	Shear stress averaged over the cardiac cycle	10,11
Oscillatory shear index (OSI)	Ratio between backward and forward going shear stress	9
Relative residence time (RRT)	Relative time that a blood particle resides at a certain location at the vessel wall	12
Transverse wall shear stress (transWSS)	Shear stress vector in perpendicular direction to the main flow direction	13
Cross-flow index (CFI)	The transWSS normalized for the time-averaged wall shear stress	14

[material online](#), *Methods*. The animal protocol was approved by the local animal ethics committee of the Erasmus MC (DEC EMC109-14-10) and the study was performed according to the National Institutes of Health guide for the care and use of Laboratory animals.<sup>19</sup> At the age of  $34 \pm 3$  months, familial-hypercholesterolaemic Bretonchelles Meishan pigs<sup>18</sup> ( $n = 10$ , castrated males) were put on a high-fat diet (10% lard and 0.75% cholesterol, the National Institute of Agronomic Research, France) that was given in restricted amounts to maintain a constant weight. At 3 months of high-fat diet ( $T_1$ ), the three-dimensional geometry of the coronary arteries was assessed by computed tomography angiography (CTA). Subsequently, an invasive imaging procedure was conducted in which near-infrared spectroscopy–intravascular ultrasound (NIRS-IVUS), and optical coherence tomography (OCT) imaging were used to assess the coronary plaque size and composition in all three main coronary arteries (i.e. left anterior descending, left circumflex, and right coronary artery). Furthermore, invasive local Doppler-derived flow velocity measurements were obtained at multiple locations in between the side branches in the coronaries. This imaging procedure was repeated at 9 ( $T_2$ ) and 10–12 months ( $T_3$ ) for all pigs. At the last imaging time point, the animals were sacrificed by an overdose of pentobarbital followed by exsanguination by removal of the heart. The coronary arteries were collected from the heart and used for histological analysis. All 3-mm coronary segments were classified according to the adjusted American Heart Association classification<sup>20</sup> [i.e. no plaque, intimal thickening, intimal xanthoma, pathological intimal thickening, and fibrous cap atheroma (FCA)]. Furthermore, the lipid, macrophage, and necrotic core content of each segment were quantified (see [Supplementary material online](#), *Methods* for more details on the staining and histological analysis methods).

For the computation of WSS at  $T_1$  and  $T_2$ , the coronary arteries were three-dimensional reconstructed by fusion of IVUS-derived lumen and wall contours of either  $T_1$  or  $T_2$ , with the three-dimensional CTA-derived centreline (see [Supplementary material online](#), *Methods* for a detailed description of three-dimensional reconstruction methodology). This resulted in a luminal surface and provided information on the local wall thickness (WT) distribution (*Figure 1A*). The reconstructed lumen surface together with the local velocity measurements served as input to compute the (multidirectional) WSS metrics at both time points, using computational fluid dynamics.

For analysis, all arteries were divided into 3-mm segments of  $45^\circ$  (sectors) (*Figure 1B*), a division that was chosen to ensure maximal overlap of the  $T_1$  and  $T_2$  data, even in the presence of small registration errors (max  $\pm 1$  IVUS frame) but at the same time to maximally account for spatial heterogeneity. For each individual artery, the WSS metrics at  $T_1$  and  $T_2$  were divided into artery-specific tertiles (low, mid, and high) ([Supplementary material online](#), *Table S1*).

IVUS data of  $T_2$  and  $T_3$  were matched based on anatomical landmarks to the IVUS data at  $T_1$  to assess, at each location, changes in plaque size (i.e. plaque growth). All data on plaque growth ( $\Delta WT \ T_1 \rightarrow T_2 = WT - T_2 - WT - T_1$ ;  $\Delta WT \ T_2 \rightarrow T_3 = WT - T_3 - WT - T_2$ ) were expressed as  $\Delta WT$  per month on high-fat diet between the respective time points. The used matching method enabled projection of  $T_2$  WSS on the  $T_1$  WSS maps, whereby permitting assessment of locations with sustained low WSS or sustained high WSS. Locations were classified as ‘sustained’ when the WSS remained either ‘low’ or ‘high’ at both  $T_1$  and  $T_2$ .

NIRS-IVUS, OCT images and histology data derived at the last imaging time point were also matched to the  $T_1$  IVUS images, again based on anatomical landmarks to establish the relationship between WSS at  $T_1$  and eventual plaque composition at the last imaging time point (see [Supplementary material online](#), *Methods* for further details).

## 2.1 Statistics

IBM SPSS Statistics (version 24.0) software was used for statistical analysis. Normally distributed data are shown as mean  $\pm$  standard deviation (SD) and statistical difference was determined with repeated measures analysis of variance with Bonferroni *post hoc* testing. Statistical differences in frequency distributions were assessed using a  $\chi^2$  test. Non-normally distributed data are presented as median (interquartile range) and statistical difference was determined with a Mann–Whitney *U* test. Statistical analysis of the relationship between plaque growth and WSS was performed using a linear mixed-effects model, with WSS (low, mid, and high), as fixed factor and the individual vessel as random factor, adjusting for cholesterol levels. The Bonferroni correction was applied to adjust for multiple comparisons between the WSS tertiles. For comparison of the WSS effect on plaque progression between  $T_1$ – $T_2$  and  $T_2$ – $T_3$ , time was added as a repeated measure factor to this same model. In all figures that display the association between plaque growth or composition and the five WSS-metrics, the estimated means and standard errors derived from these models are displayed. A *P*-value  $< 0.05$  was regarded as significant.

## 3. Results

Of the 10 pigs, one pig died during feeding, a day after the invasive imaging procedure at  $T_2$ , due to a presumed myocardial infarction. One pig had to be sacrificed between  $T_2$  and  $T_3$  due to an acute thrombotic occlusion of a femoral artery. Data of these pigs have been included in the analysis; although imaging information at  $T_3$  is missing. For analysis of the relation between  $T_1$  WSS metrics and eventual plaque composition,  $T_2$  was considered as  $T_{\text{last}}$  for these two pigs. For the other pigs,  $T_3$  equalled  $T_{\text{last}}$ . In total, 30 vessels relating to 3648 3 mm/ $45^\circ$  sectors were analysed.

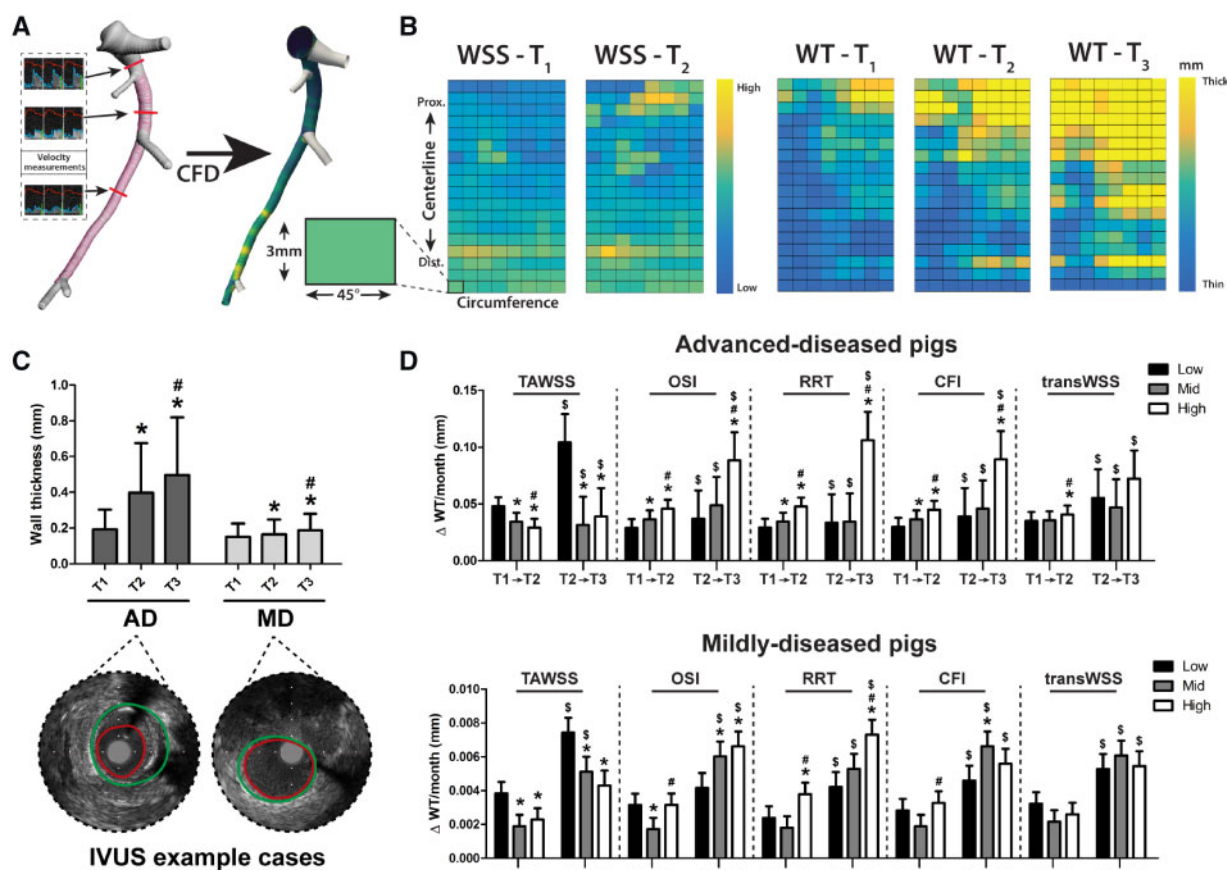


**Figure 1** Methodology of WSS calculation and analysis, and the relationship between local (multidirectional) WSS levels and the subsequent plaque growth rate in both plaque initiation and progression. (A) IVUS (pink) and computed tomography (white) contours were fused to reconstruct the grey lumen surface. This surface, together with local flow measurements between the side branches (three examples shown), was used as input for computational fluid dynamics (CFD), resulting in local WSS values (yellow = high; blue = low). (B) From the three-dimensional reconstructions, a two-dimensional map of the WSS levels at T<sub>1</sub> and T<sub>2</sub> and of the WT (T<sub>1</sub>–T<sub>3</sub>) was created. For the analysis, the artery was divided in 3 mm/45° sectors. (C) The mean (±SD) WT at T<sub>1</sub>–T<sub>3</sub> in advanced-diseased (AD) (*n* = 1893 sectors at T<sub>1</sub> and T<sub>2</sub> and *n* = 1240 sectors at T<sub>3</sub>) and mildly-diseased (MD) (*n* = 1755 sectors) pigs with two representative IVUS frames from T<sub>3</sub> (red contour = lumen; green contour = vessel wall). \**P* < 0.05 compared to T<sub>1</sub>, #*P* < 0.05 compared to T<sub>2</sub> (statistics: two-way repeated-measures analysis of variance with Bonferroni *post hoc*). (D) The effect of low/mid/high levels of the respective WSS metrics on the subsequent plaque growth rate (estimated mean ± SEM) in plaque initiation (T<sub>1</sub>–T<sub>2</sub>) and plaque progression (T<sub>2</sub>–T<sub>3</sub>). Important to note: for the AD pigs, the T<sub>2</sub>–T<sub>3</sub> data are derived from three (instead of five) pigs (*n* = 1240 sectors), which means that the analysis of a difference in the relation between T<sub>1</sub>–T<sub>2</sub> and T<sub>2</sub>–T<sub>3</sub> (§) could only be performed in these three animals. \**P* < 0.05 compared to the low tertile; #*P* < 0.05 compared to the mid tertile; §*P* < 0.05 compared to T<sub>1</sub>–T<sub>2</sub> in the same tertile (statistics: linear mixed effects model). CFI, cross-flow index; OSI, oscillatory shear index; RRT, relative-residence time; TAWSS, time-averaged WSS; transWSS, transverse WSS.

### 3.1 Advanced-diseased and mildly-diseased pigs

Although all pigs had the same mutation and were fed the same diet, five of the 10 pigs developed large, lumen intruding coronary plaques [plaque burden (PB) >40%] [advanced-diseased pigs, ADs] within 9 months, while the other five pigs only developed limited atherosclerosis (PB < 40%) within 12 months of follow-up (mildly-diseased pigs, MDs). The observed PB at the last imaging time point was 35% (12–77%) for the ADs and 16% (8–34%) for the MDs [median (range)]. The two groups of pigs showed no difference in weight [MDs: 91 kg (80–94) vs. ADs 82 kg (68–94) (*P* = 0.33)] and in cholesterol, LDL, HDL levels [10.4 mmol/L (9.2–12.1) vs. 10.5 mmol/L (9.8–18.3) (*P* = 0.54); 2.8 mmol/L (2.5–4.2) vs. 3.0 mmol/L (2.3–3.5) (*P* = 0.79); 8.5 mmol/L (7.1–9.8) vs.

9.2 mmol/L (8.1–16.6) (*P* = 0.33) in MD vs. AD, respectively]. Because of the large difference in plaque development, the subsequent results will be presented separately for both groups.

### 3.2 Low and multidirectional WSS result in a high coronary plaque growth rate, both in plaque initiation and plaque progression

Overall, the ADs demonstrated a significant increase of the average WT over the three imaging time points (T<sub>1</sub>–T<sub>3</sub>) (*P* < 0.001), which was less pronounced, but also significant in the MDs (*P* < 0.001) (Figure 1C). There was no difference in absolute WSS values between the AD and MD pigs at T<sub>1</sub>. At T<sub>2</sub>, the OSI, RRT, and CFI levels were slightly higher in the MD than in the AD pigs (Supplementary material online, Table S1).



In general, the plaque growth rate was higher between  $T_2$  and  $T_3$  than between  $T_1$  and  $T_2$  for both AD and MD pigs (Figure 1D).

In the AD pigs, coronary sectors exposed to low TAWSS or high multidirectional WSS (OSI, RRT, CFI, or transWSS) at  $T_1$  exhibited a significantly higher initial plaque growth per month between  $T_1$  and  $T_2$  than regions with higher (TAWSS) or lower (multidirectional metrics) WSS levels ( $P < 0.05$ ). The same significant relations were seen for the plaque progression rate ( $T_2$ – $T_3$ ), except for the transWSS (Figure 1D). Also in the MDs, low TAWSS and high RRT levels were related to the fastest initial plaque growth ( $T_1$ – $T_2$ ) and plaque progression ( $T_2$ – $T_3$ ). High OSI levels promoted plaque progression, but not initiation in the MDs. For CFI and transWSS, no relation with plaque growth was observed in the MDs (Figure 1D).

Besides the effect of WSS values at a single time point, we also assessed what the relation was between sustained low or high WSS and the plaque growth rate during plaque initiation and progression. In plaque initiation, in the ADs, the plaque growth rate was highest in regions with initial ( $T_1$ ) low TAWSS, that over time changed to high TAWSS (at  $T_2$ ) ( $\Delta WT$   $T_1 \rightarrow T_2$ :  $0.073 \pm 0.008$  mm/month;  $n = 94$ , 5%), also compared to regions with persistently low TAWSS ( $0.038 \pm 0.008$  mm/month;  $n = 361$ , 19%) (Figure 2). Besides, also regions with initial ( $T_1$ ) high OSI, RRT, or CFI and subsequently ( $T_2$ ) low multidirectional WSS presented with the highest plaque growth rate. For the MD pigs, similar results were obtained, but only for the TAWSS and RRT. Subsequently, we assessed in these same regions what the plaque progression was between  $T_2$  and  $T_3$ . Both in the ADs and MDs, in regions with initial low and subsequently high TAWSS, the plaque growth rate between  $T_2$  and  $T_3$  was lowest (Figure 2). The highest plaque progression rate was observed in regions with low TAWSS at  $T_2$ , independent of the  $T_1$  TAWSS levels. For the multidirectional WSS metrics, no clear relations were observed between sustained WSS and the plaque growth rate ( $T_2$ – $T_3$ ), except for low RRT levels at  $T_2$  which appeared leading in very limited plaque growth.

The positive predictive values (PPVs) of the  $T_1$  WSS metrics for plaque presence ( $WT > 0.5$  mm) at  $T_{last}$  in the AD pigs were 48% (low TAWSS), 45% (high OSI), 47% (high RRT), 45% (high CFI), and 40% (high transWSS). Regions with low TAWSS co-locate with high OSI in 396/624 sectors (63%). Co-localization of low TAWSS and high CFI occurs in 354/624 sectors (57%). Combination of low TAWSS and high OSI resulted in a PPV of 50% for plaque presence. The PPV for low TAWSS and high CFI for plaque presence was 49%. The combination of all three metrics resulted in a PPV of 50%. In the MD pigs, a predictive value analysis could not be applied since only six sectors (of the total of 1755 sectors) presented with a  $WT > 0.5$  mm at  $T_{last}$ .

### 3.3 The development of OCT lipid-rich plaques and NIRS-positive plaques was most often preceded by low and multidirectional WSS

Analysis of the NIRS signal at  $T_{last}$  (Figure 3A) showed that the MDs presented with only six NIRS-positive sectors from three different arteries, while the ADs demonstrated 33 NIRS-positive sectors derived from six arteries. The NIRS positive sectors of the ADs were most frequently preceded by low TAWSS ( $P = 0.10$ ), or high OSI ( $P < 0.05$ ), RRT ( $P = 0.08$ ) or CFI ( $P < 0.05$ ) at  $T_1$  (Figure 3B). Only transWSS showed no relation at all with NIRS-positive plaque development in the ADs.

For the OCT analysis (Figure 3A), two pullbacks from  $T_{last}$  had to be excluded due to bad image quality or technical problems. From the

remaining pullbacks at  $T_{last}$ , 668 sectors from 14 arteries of the ADs and 66 sectors from 10 arteries of the MDs showed plaque presence. In the ADs, the plaque positive sectors were characterized as either a fibrous ( $n = 196$ ), lipid-rich ( $n = 469$ ), or OCT-detected FCA (lipid-pool) ( $n = 3$ ) plaque (Figure 3C). Since the OCT-FCAs (with lipid-pool) were scarce, no statistical analysis and thus no WSS analysis could be performed on this plaque type. The development of a fibrous plaque showed no relation with  $T_1$  WSS levels in both types of pigs (Figure 3D and Supplementary material online, Figure S1). In contrast, the development of OCT lipid-rich plaques was most frequently preceded by low and multidirectional WSS in the ADs ( $P < 0.05$ ) (Figure 3D). This relation was confirmed for OSI, CFI, and transWSS in the MDs, despite the low number of lipid-rich plaques in this group ( $n = 45$ ) (Supplementary material online, Figure S1).

### 3.4 Low and multidirectional WSS promoted the development of advanced histological plaque types

For a detailed analysis of the association between histological plaque classification, composition, and  $T_1$  WSS levels, 190 3-mm segments (15 arteries) from ADs and 145 3-mm segments (13 arteries) derived from MDs could be reliably matched with the invasive imaging data. In the MDs, of all WSS metrics, only TAWSS showed a significant association with histological plaque type, with relatively the most advanced plaques in regions with low TAWSS compared to regions with mid- or high TAWSS ( $P = 0.049$ ) (Supplementary material online, Figure S2A and B). In the ADs, this TAWSS relation was more pronounced ( $P = 0.003$ ), and also regions with high OSI and high RRT displayed a more advanced plaque phenotype than regions with lower OSI or RRT levels ( $P < 0.05$ ). For transWSS and CFI, no relation with plaque type was observed (Figure 4B). The PPVs of the respective WSS metrics for the presence of an FCA in the ADs were 61% (low TAWSS), 58% (high OSI), 61% (high RRT), 59% (high CFI), and 49% (high transWSS).

A more detailed analysis of the plaque composition in the ADs supported these results. We observed that in regions with low (TAWSS) and multidirectional WSS (RRT and CFI), plaques presented with the largest lipid and macrophage area ( $P < 0.05$ ) (Figure 5A and B). High OSI levels showed a positive trend for increased lipid content. For the necrotic core area, low TAWSS and high RRT levels resulted in twice as large necrotic cores compared to regions with higher TAWSS or lower RRT (Figure 5C). TransWSS showed no relation with plaque composition ( $P = NS$ ). For the MDs, no significant relation was observed between any of the WSS metrics and plaque composition (Supplementary material online, Figure 2C).

## 4. Discussion

In the present study, we used a serial, multimodality imaging protocol in conjunction with histological analyses to assess the influence of (multidirectional) WSS on the natural initiation and progression of coronary atherosclerotic plaques in a unique adult familial hypercholesterolaemia pig model. This study design enabled for the first time a comprehensive comparison of five (multidirectional) WSS metrics for their influence on plaque progression and composition changes. The results of the study are summarized in Table 2 and demonstrated that: (i) plaque initiation and plaque progression are associated with low TAWSS and high levels of multidirectional WSS, both in mildly-diseased and advanced-diseased pigs, with the most pronounced relations in the latter group; (ii) the

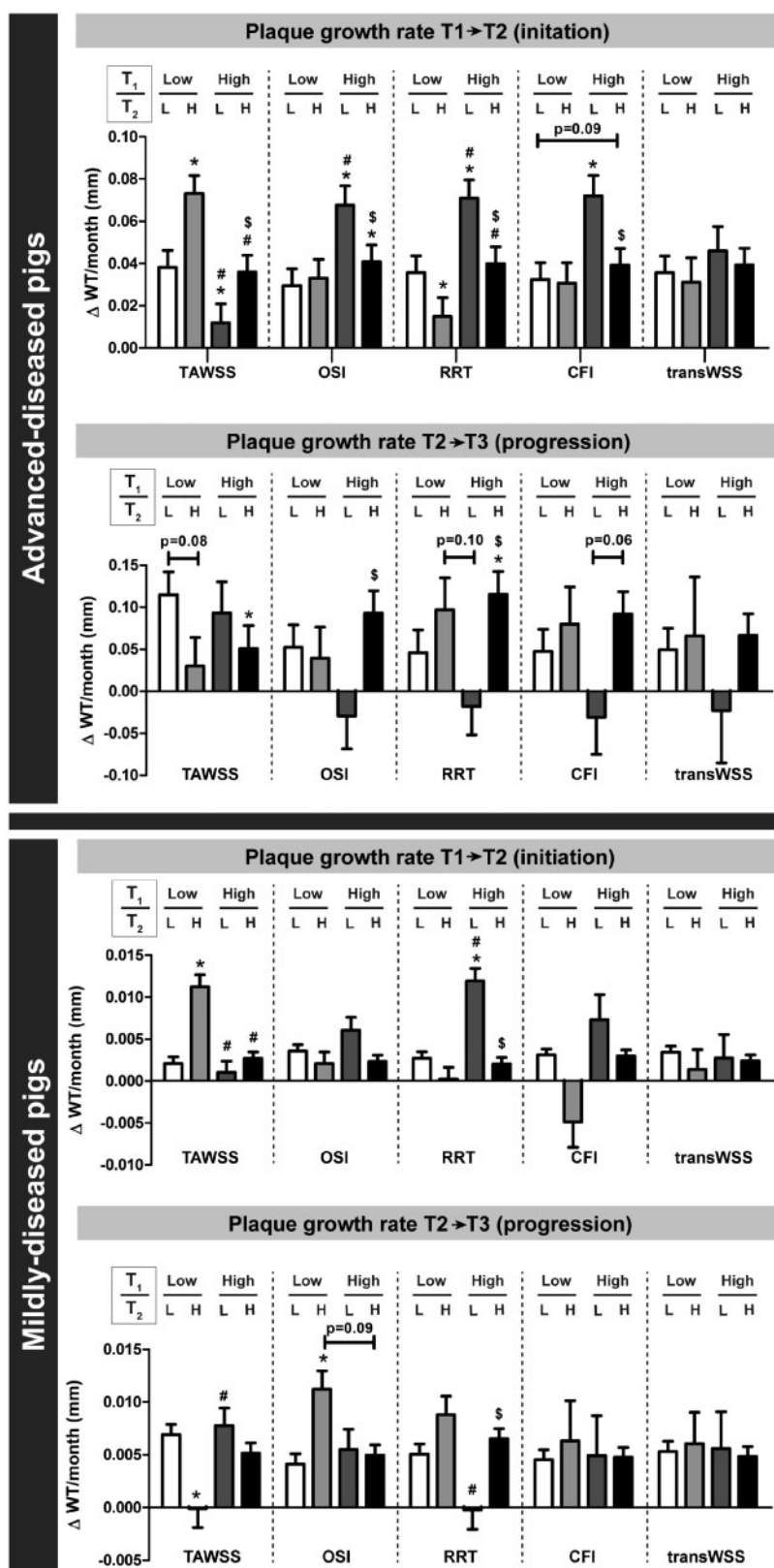


**Figure 2** The long-term effect of sustained or changed levels of (multidirectional) WSS on the plaque growth rate in advanced-diseased (AD) and mildly-diseased (MD) pigs. The plaque growth rate during plaque initiation (T<sub>1</sub>→T<sub>2</sub>) and plaque progression (T<sub>2</sub>→T<sub>3</sub>) in regions with either sustained low (L), low turning to high (H), high turning to low, or sustained high WSS between T<sub>1</sub> and T<sub>2</sub>. Analysis is depicted for all WSS metrics [TAWSS, OSI, RRT, CFI, and transWSS]. Number of analysed sectors: for AD pigs T<sub>1</sub>→T<sub>2</sub>: *n* = 1893 and T<sub>2</sub>→T<sub>3</sub>: *n* = 1240; for MD pigs: *n* = 1755. \**P* < 0.05 compared to sustained low; #*P* < 0.05 compared to low (T<sub>1</sub>)/high (T<sub>2</sub>); \$*P* < 0.05 compared to high (T<sub>1</sub>)/low (T<sub>2</sub>) (statistics: linear mixed effects model).

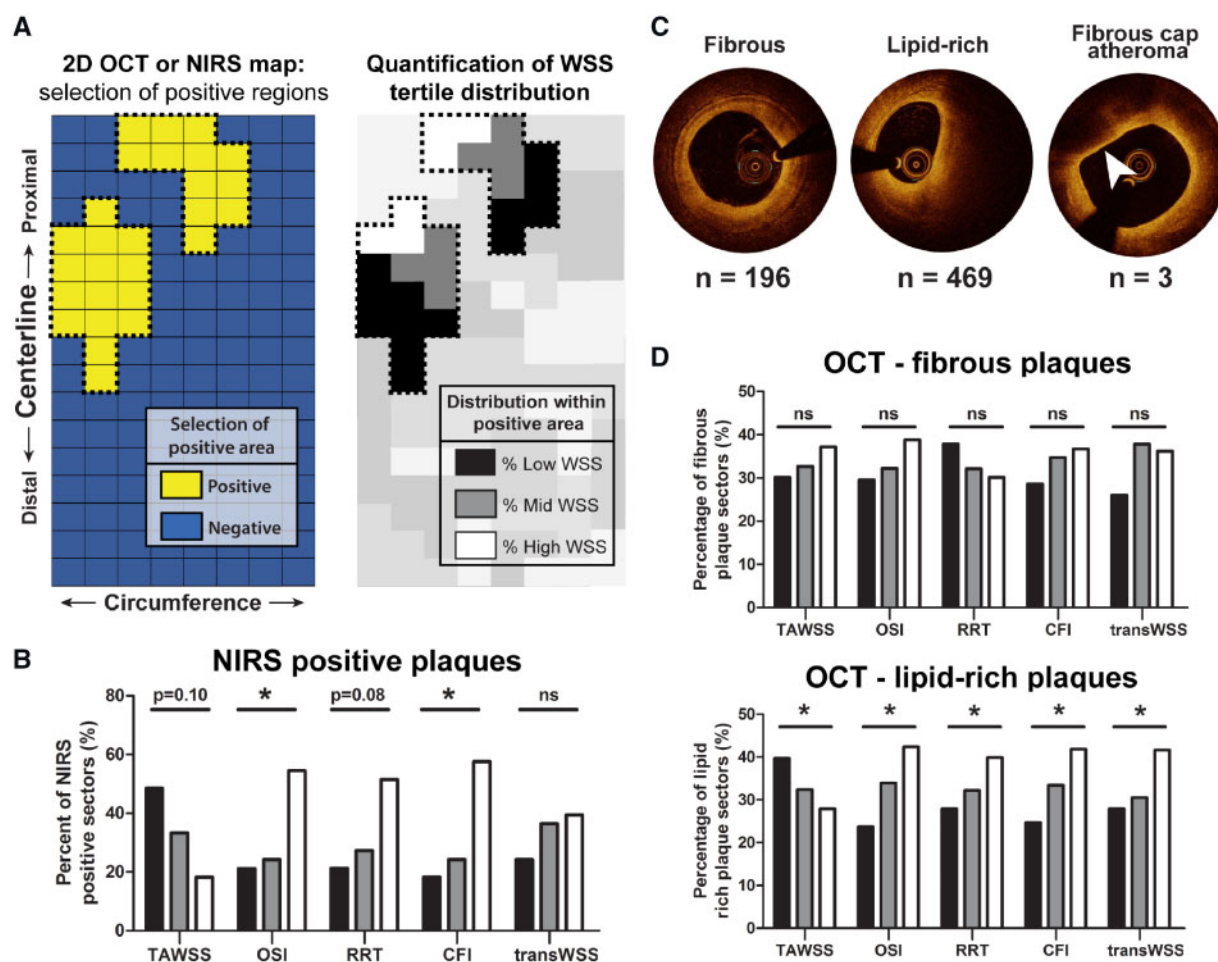


**Figure 3** Association between  $T_1$  WSS levels and final plaque composition detected by OCT and NIRS in advanced-diseased (AD) pigs at  $T_{last}$ . (A) OCT and NIRS analysis method on an imaginary two-dimensional map: all NIRS or OCT positive  $3\text{ mm}/45^\circ$  sectors were selected. Within these positive regions, the percentage of positive sectors that was preceded by one of the WSS tertiles was quantified. (B) The percentage of NIRS-positive sectors ( $n = 33$ ) that was preceded by low (black bars), mid (grey bars), or high (white bars) levels of the respective  $T_1$  WSS tertiles (TAWSS, OSI, RRT, CFI, and transWSS). \* $P < 0.05$  for the overall relations (statistics:  $\chi^2$  test). (C) Example images of fibrous, lipid-rich, and fibrous cap atheroma (arrowhead) plaques on OCT.  $n$ , number of sectors of ADs presenting with each respective plaque classification at  $T_{last}$ . (D) The percentage of sectors presenting with fibrous or lipid-rich plaque that was preceded by low (black bars), mid (grey bars), or high (white bars) levels of the respective WSS metrics. Fibrous plaques displayed no significant relation ( $P = ns$ ). \* $P < 0.05$  for the overall relations (statistics:  $\chi^2$  test).

greatest plaque growth rate was observed in regions with initial low TAWSS, turning into high TAWSS at  $T_2$ , while for multidirectional WSS, no clear differences in plaque growth rate were observed between regions with either sustained or changing WSS levels; (iii) plaques with a vulnerable composition, as observed in the AD pigs, most often developed in regions with low TAWSS and high levels of OSI, RRT, and CFI, while transWSS was not related to plaque composition; and (iv) all multidirectional WSS metrics, except transWSS, have a good PPV for development of plaque, and an even better predictive value for the development of FCA.

#### 4.1 Relation of low and multidirectional WSS with plaque initiation, progression, and composition

In order to discuss our results on the relationship between WSS and plaque initiation and progression, it is vital to recognize the different roles

of WSS in the various stages of atherosclerosis.<sup>10</sup> In clinical studies, the presence of larger stenosis degrees leads to local elevation of the WSS. In these advanced disease stages, WSS, in combination with intravascular imaging to detect plaque composition, could serve as a marker for localizing vulnerable plaques, or form a predictor for plaque destabilization as suggested by the studies of Kumar *et al.*<sup>21</sup> and Slager *et al.*<sup>22</sup> Pre-clinical studies, or clinical studies that exclude narrowed arterial regions, are the only way to assess the causal role of WSS in plaque initiation and progression. In this discussion, considering our study design, we focused on the role of (multidirectional) WSS in early disease development.

Absolute WSS levels are highly dependent on the used methodology, which for example results in the, on average, lower TAWSS values in our study compared to most of the previously reported absolute values. This is most likely caused by the fact that side branches were included in our models, which lowers the flow and thus the WSS through the downstream artery. Because of this methodological dependency, a reliable



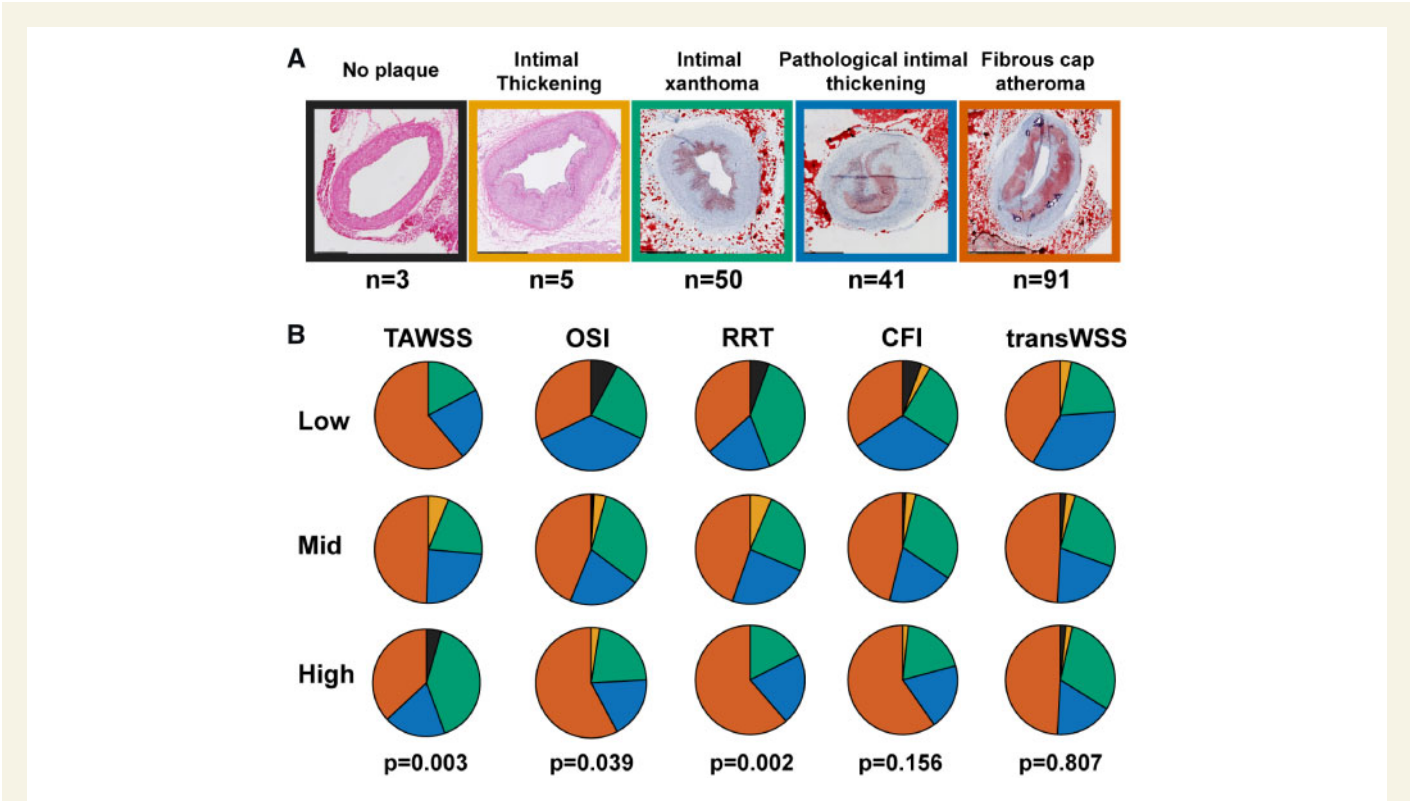


**Figure 4** Relation between histological plaque classification and  $T_1$  (multidirectional) WSS levels in the advanced-disease pigs. (A) Histological examples of plaques according to the revised American Heart Association plaque classification. (B) Distribution of the plaque types over regions with preceding low, mid, or high levels of the respective WSS metrics (TAWSS, OSI, RRT, CFI, and transWSS).  $P$ -value is for the overall relations (statistics:  $\chi^2$  test).

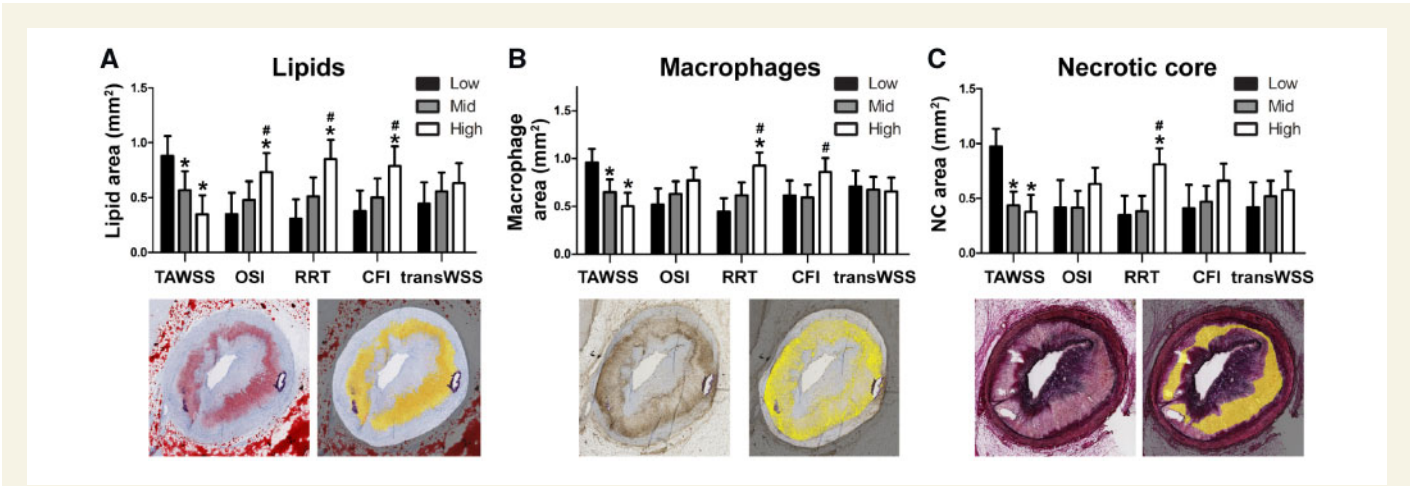


**Figure 5** The effect of  $T_1$  (multidirectional) WSS levels on final histological plaque composition in advanced-diseased pigs. (A–C) The absolute lipid (Oil-red-O staining, red = lipid) (A), macrophage (CD68 staining, brown = macrophages) (B) or necrotic core (Miller staining, purple = collagen) (C) area (example positive staining indicated in yellow) preceded by low, mid, or high levels of one of the five WSS metrics (mean  $\pm$  SD) (TAWSS, OSI, RRT, CFI, and transWSS). \* $P < 0.05$  vs. low tertile of the respective WSS metric; # $P < 0.05$  vs. mid tertile (statistics: linear mixed effects model).

comparison of the relation between different multidirectional WSS metrics and plaque development is only possible within one study. With our current study, we are the first to assess and compare the effect of five different (multidirectional) WSS metrics on plaque initiation and progression. We confirmed the findings from previous studies<sup>2,9,23</sup> which

showed that low TAWSS and high levels of OSI and RRT result in the highest initial plaque growth. We also observed that the same relation holds true for plaque progression. Both CFI and transWSS showed similar, but less pronounced relations with plaque initiation and progression.



**Table 2** Overview of all WSS metrics that influence plaque growth or plaque composition

	Advanced-diseased pigs	Mildly-diseased pigs
Plaque growth rate (initiation phase)	Low TAWSS	Low TAWSS
	High OSI, RRT, or CFI	High RRT
	Sustained low TAWSS	Sustained low TAWSS
	Sustained high OSI or RRT	Sustained high RRT
Plaque growth rate (progression phase)	Low TAWSS	Low TAWSS
	High OSI, RRT, or CFI	High OSI or RRT
Advanced plaque composition	Low TAWSS	Low TAWSS
	High OSI or RRT	
Lipid abundance	Low TAWSS	No relationship
	High OSI, RRT, or CFI	
Macrophage abundance	Low TAWSS	No relationship
	High RRT	
Necrotic core size	Low TAWSS	n/a
	High RRT	

As already described in a study by Koskinas et al.,<sup>24</sup> WSS levels change over time. We observed that around 48% of the studied segments exhibited changes in local WSS levels. With regard to plaque initiation, the largest plaque growth was found in sectors with T<sub>1</sub> low TAWSS that changed to higher TAWSS at T<sub>2</sub>. This local elevation of TAWSS at T<sub>2</sub> can very well be caused by lumen intrusion of large plaques, which was similarly observed in human advanced disease by Kumar et al.<sup>21</sup> Interestingly, in these same regions with high TAWSS at T<sub>2</sub>, the plaque growth rate during plaque progression between T<sub>2</sub> and T<sub>3</sub> was lowest of all analysed sectors. This could indicate that the growth rate of these large plaques tends to decrease when the TAWSS rises. Despite the relatively short-time period between T<sub>2</sub> and T<sub>3</sub>, the significantly highest plaque growth rate from T<sub>2</sub> to T<sub>3</sub> was observed in regions with low TAWSS at T<sub>2</sub>, independent from the TAWSS levels at T<sub>1</sub>. Apparently, when low WSS is present, it triggers plaque growth, confirming the findings by Koskinas et al.,<sup>24</sup> until the plaque starts to intrude into the lumen and TAWSS levels elevate. For the multidirectional WSS parameters OSI, RRT, and CFI, regions with initial (T<sub>1</sub>) high and subsequently (T<sub>2</sub>) low levels presented with the highest plaque growth rate. Although never studied before, this could mean that the multidirectionality of WSS reduces upon plaque lumen intrusion. This reduced multidirectionality then results in reduced plaque growth as observed in our plaque progression (T<sub>2</sub>–T<sub>3</sub>) analysis.

Not only plaque size, but also plaque composition is important for risk-assessment of coronary events.<sup>25</sup> In two human studies with advanced disease, a correlation has been shown between (the development of) a positive NIRS signal (i.e. lipid-rich plaques) and high TAWSS.<sup>26,27</sup> Such a relation has never been described for earlier disease stages. In this study, we demonstrated a trend between NIRS-positive plaques and preceding low TAWSS. Multidirectional WSS metrics showed an even stronger effect, with NIRS-positive plaque development significantly more often preceded by high OSI and CFI levels compared to low multidirectional WSS. However, since the number and size of NIRS-positive regions was limited, our results on the correlation between WSS and NIRS should be interpreted with care.

The observed relation between (multidirectional) WSS and lipid-rich plaques derived from NIRS imaging was confirmed by OCT. Important to notice is that the number of OCT-detected FCAs was much lower compared to our histological findings. Reassessment of the accompanying histological data revealed that many lipid-rich necrotic cores are apparently invisible on OCT, hypothetically because they are ‘shielded’ by a layer of lipids in the cap structure.

Previous pre-clinical studies applied histology to determine the relation between plaque composition and WSS. These studies demonstrated that the development of advanced plaques with lipid and inflammatory cell infiltration was associated with low TAWSS.<sup>2,17,23,28</sup> Furthermore, Pedrigi et al.,<sup>17</sup> who used a perivascular cuff to induce atherosclerosis formation, concluded that, besides low WSS, also a variant metric of the transWSS was associated with advanced plaques. In our study, we demonstrated with histology that advanced plaques with a higher lipid and inflammatory cell content and larger necrotic cores developed in regions with low WSS, confirming the results from the previous studies.<sup>2,17,23,28</sup> In contrast to the findings by Pedrigi et al.,<sup>17</sup> transWSS was not related to plaque composition. This difference might be related to the use of the perivascular cuff in the study of Pedrigi. The narrowing of the vessel induced by this cuff can result in multidirectional flow patterns that are normally not observed in early disease stages. However, we did show that the multidirectional metric RRT was strongly associated with the development of plaques with an advanced and complex composition. High levels of OSI and CFI mainly co-localized with regions with an overall more advanced plaque phenotype and with a high lipid-content, but could not be related to macrophage abundance or necrotic core size. Following these observations, plaque inflammation might mainly be affected by low WSS resulting in a high particle-residence time (RRT), but not by more complex flow patterns expressed by the OSI and CFI.

Although shear stress is known to influence plaque composition over time, thereby also affects the risk on plaque rupture, analysis of the structural stress in the vessel wall better predict the immediate risk on cardiovascular events. Wall stress can be assessed using computational modelling with the plaque composition and loading conditions as input.<sup>29</sup> Recently, more advanced methodologies have been applied, such as fluid-structure interaction, but these methods require input on often unknown boundary conditions.<sup>30,31</sup>

Many of our above-mentioned findings were most pronounced in our advanced-diseased pigs, while in our mildly-diseased pigs, mainly the TAWSS and the RRT were associated with plaque development. The observed differences between MD and AD pigs will be discussed below.

**4.2 Advanced and mildly diseased pigs: difference in plaque growth and response to WSS metrics**

We observed clear differences in plaque size and growth, but also in the response to WSS between MD and AD animals, despite similar WSS levels and conventional risk factors. The difference in response to WSS between the ADs and MDs indicates that, as commonly accepted, besides WSS, more factors are (synergistically) involved in determining the sensitivity for plaque development. As discovered in a previous study by our group (Hoogendoorn et al., unpublished data, 2019), a pronounced difference in low-density lipoprotein profile between the ADs and MDs makes the AD pigs much more prone to develop (coronary) atherosclerosis. Recent publications confirm these findings and show that, also in patients, differences in specific lipoprotein profiles can result in

inter-individual differences in cardiovascular outcome.<sup>32,33</sup> Since WSS is mainly a factor that triggers the local influx of inflammatory cells and lipids into the vessel wall in an already high-risk systemic environment, differences in systemic risk factors like the low-density lipoprotein profile might explain why WSS in the MDs is not as strongly associated with plaque growth as in the ADs. However, despite a systemic predisposition for plaque growth in the AD pigs, plaque development and progression were strongly related to shear stress in both groups of pigs, implying an essential role for shear stress in plaque development.

Unfortunately, comparison of these results with other pre-clinical WSS literature is difficult, since animals that present with limited plaque growth are regarded as 'non-responders' and are often not taken into account for analysis. To make an honest assessment of the role of WSS in plaque development, thereby also better mimicking the large variability in disease development observed in human populations, we retained the MD pigs in the analysis.

### 4.3 The predictive value of multidirectional WSS metrics

To enable the future application of WSS measurements in the clinic, establishing its PPV for plaque progression is important. The PREDICTION study<sup>5</sup> reported a PPV of low TAWSS of 25% in comparison to 50% in our study. The higher PPV in our study could, at least in part, be explained by the fact that, in contrast to all PREDICTION patients, our animals did not receive statin treatment which is known to induce plaque regression. In stable ACS patients, Rikhtegar *et al.*<sup>12</sup> reported that multidirectional WSS parameters might be a better predictor for plaque localization at one-time point than low TAWSS (low TAWSS: 31%; high OSI: 35%; high RRT: 49%). In our study, where the effect of WSS metrics on plaque development over time was assessed, we show that low TAWSS and high RRT are the best predictors, partially contrasting the results of Rikhtegar *et al.* Finally, while most studies have evaluated the PPV of WSS for plaque size, we are the first to assess the predictive value of WSS for plaque composition. Interestingly, we observed that WSS might be an even better predictor for the development of FCA than for plaque size [PPV of 61% (TAWSS and RRT) vs. 50% (TAWSS) and 49% (RRT)]. With this study, we enabled, for the first time, a reliable one-to-one comparison of five different WSS metrics for plaque development. Based on our results, we can now conclude that, although multidirectional WSS is significantly involved in the disease process, low TAWSS remains the strongest driving factor and predictor of both plaque initiation and progression. This finding could offer an advantage with regard to computational times since TAWSS can reliably be approached by stationary simulations.<sup>34</sup> These stationary simulations are much less time-consuming than full time-dependent simulations that are needed for multidirectional WSS calculations.

### 4.4 Limitations

The present study has a number of limitations. First, the coronary arteries were modelled as static non-moving arteries. We showed in an earlier study that shear stress in a natural moving and deforming coronary artery is well approximated by modelling steady mean flow in the rigid diastolic geometry of this coronary artery.<sup>35</sup> Second, the number of pigs used in this study was small, and the unexpected split into advanced- and mildly-diseased animals further reduced the number of arteries that were available to investigate advanced plaque development. However, multiple sectors within one coronary artery were analysed to capture the local WSS effect. A linear mixed-effects model was applied to correct for remaining

dependencies. Using this approach, a statistically significant effect of multidirectional WSS on plaque development could be identified in both types of pigs. Furthermore, since the absolute levels of OSI, CFI and transWSS were low, the division of the WSS tertiles could be considered as somewhat artificial. Still, we did find significant relations between the relative levels of these metrics and both plaque size and composition.

## 5. Conclusion

In the present study, we combined detailed invasive imaging and histopathology to demonstrate that the highest plaque growth rate was exclusively found at low TAWSS or high multidirectional WSS at both  $T_1$  (for plaque initiation) and  $T_2$  (for plaque progression). Regions with initial low TAWSS which, over time, turned into regions with high TAWSS, demonstrated the overall largest plaque growth. For multidirectional WSS, the largest plaque growth was found in regions with initial high levels of OSI, RRT, and CFI that changed into regions with low levels of these parameters. These elevated TAWSS levels and reduced multidirectional WSS levels at  $T_2$  are probably due to the development of lumen-intruding plaques. The development of plaques with an advanced plaque composition was also related to low TAWSS and high OSI, RRT or CFI, but not to transWSS. While the predictive values of the individual multidirectional WSS metrics for plaque growth were high, advanced plaque composition was even more reliably predicted by (multidirectional) WSS metrics with the TAWSS and RRT being the strongest predictors. The differences between the AD and MD pigs stress the importance of a synergistic effect of systemic risk factors and local shear stress levels. The overall results highlight that, although multidirectional WSS is significantly involved in coronary plaque initiation and progression, low TAWSS remains the best predictive clinical marker for the vulnerable disease development.

## Supplementary material

Supplementary material is available at *Cardiovascular Research* online.

## Acknowledgements

We gratefully acknowledge Ilona Krabbendam—Peters, Karen Witberg, Maaike Visser—te Lintel Hekkert, Kim van Gaalen, Jurgen Ligthart, and Marcel Dijkshoorn for their expert technical assistance in the animal experiments and data acquisition. Furthermore, we thank Maria Siebes for the lending of the ComboMap device and the accompanying user-advice.

**Conflict of interest:** none declared.

## Funding

This work was supported by the European Research Council, Brussels, Belgium [grant number 310457].

## References

- Mathers CD, Loncar D. Projections of global mortality and burden of disease from 2002 to 2030. *PLoS Med* 2006;3:e442.
- Chatzizisis YS, Jonas M, Coskun AU, Beigel R, Stone BV, Maynard C, Gerrity RG, Daley W, Rogers C, Edelman ER, Feldman CL, Stone PH. Prediction of the localization of high-risk coronary atherosclerotic plaques on the basis of low endothelial

- shear stress—an intravascular ultrasound and histopathology natural history study. *Circulation* 2008;**117**:993–1002.
3. Koskinas KC, Chatzizisis YS, Papafakis MI, Coskun AU, Baker AB, Jarolim P, Antoniadis A, Edelman ER, Stone PH, Feldman CL. Synergistic effect of local endothelial shear stress and systemic hypercholesterolemia on coronary atherosclerotic plaque progression and composition in pigs. *Int J Cardiol* 2013;**169**:394–401.
  4. Koskinas KC, Chatzizisis YS, Baker AB, Edelman ER, Stone PH, Feldman CL. The role of low endothelial shear stress in the conversion of atherosclerotic lesions from stable to unstable plaque. *Curr Opin Cardiol* 2009;**24**:580–590.
  5. Stone PH, Saito S, Takahashi S, Makita Y, Nakamura S, Kawasaki T, Takahashi A, Katsuki T, Nakamura S, Namiki A, Hirohata A, Matsumura T, Yamazaki S, Yokoi H, Tanaka S, Otsuji S, Yoshimachi F, Honye J, Harwood D, Reitman M, Coskun AU, Papafakis MI, Feldman CL; PREDICTION Investigators. Prediction of progression of coronary artery disease and clinical outcomes using vascular profiling of endothelial shear stress and arterial plaque characteristics: the PREDICTION Study. *Circulation* 2012;**126**:172–181.
  6. Stone PH, Maehara A, Coskun AU, Maynard CC, Zaromytidou M, Siasos G, Andreou I, Fotiadis D, Stefanou K, Papafakis M, Michalis L, Lansky AJ, Mintz GS, Serruys PW, Feldman CL, Stone GW. Role of low endothelial shear stress and plaque characteristics in the prediction of nonculprit major adverse cardiac events: the PROSPECT study. *JACC Cardiovasc Imaging* 2018;**11**:462–471.
  7. Corban MT, Eshtehardi P, Suo J, McDaniel MC, Timmins LH, Rassoul-Arzumly E, Maynard C, Mekonnen G, King S, Quyyumi AA, Giddens DP, Samady H. Combination of plaque burden, wall shear stress, and plaque phenotype has incremental value for prediction of coronary atherosclerotic plaque progression and vulnerability. *Atherosclerosis* 2014;**232**:271–276.
  8. Samady H, Eshtehardi P, McDaniel MC, Suo J, Dhawan SS, Maynard C, Timmins LH, Quyyumi A, Giddens DP. Coronary artery wall shear stress is associated with progression and transformation of atherosclerotic plaque and arterial remodeling in patients with coronary artery disease/clinical perspective. *Circulation* 2011;**124**:779–788.
  9. Peiffer V, Sherwin SJ, Weinberg PD. Does low and oscillatory wall shear stress correlate spatially with early atherosclerosis? A systematic review. *Cardiovasc Res* 2013;**99**:242–250.
  10. Wentzel JJ, Chatzizisis YS, Gijsen FJH, Giannoglou GD, Feldman CL, Stone PH. Endothelial shear stress in the evolution of coronary atherosclerotic plaque and vascular remodelling: current understanding and remaining questions. *Cardiovasc Res* 2012;**96**:234–243.
  11. Cunningham KS, Gotlieb AI. The role of shear stress in the pathogenesis of atherosclerosis. *Lab Invest* 2005;**85**:9–23.
  12. Rikhtegar F, Knight JA, Olgac U, Saur SC, Poulikakos D, Marshall W, Cattin PC, Alkadhi H, Kurtcuoglu V. Choosing the optimal wall shear parameter for the prediction of plaque location—A patient-specific computational study in human left coronary arteries. *Atherosclerosis* 2012;**221**:432–437.
  13. Peiffer V, Sherwin SJ, Weinberg PD. Computation in the rabbit aorta of a new metric—the transverse wall shear stress—to quantify the multidirectional character of disturbed blood flow. *J Biomech* 2013;**46**:2651–2658.
  14. Mohamied Y, Sherwin SJ, Weinberg PD. Understanding the fluid mechanics behind transverse wall shear stress. *J Biomech* 2017;**50**:102–109.
  15. Knight J, Olgac U, Saur SC, Poulikakos D, Marshall W, Cattin PC, Alkadhi H, Kurtcuoglu V. Choosing the optimal wall shear parameter for the prediction of plaque location—a patient-specific computational study in human right coronary arteries. *Atherosclerosis* 2010;**211**:445–450.
  16. Timmins LH, Molony DS, Eshtehardi P, McDaniel MC, Oshinski JN, Giddens DP, Samady H. Oscillatory wall shear stress is a dominant flow characteristic affecting lesion progression patterns and plaque vulnerability in patients with coronary artery disease. *J R Soc Interface* 2017;**14**:20160972.
  17. Pedrigi RM, Poulsen CB, Mehta VV, Ramsing Holm N, Pareek N, Post AL, Kilic ID, Banya WAS, Dall'Ara G, Mattesini A, Björklund MM, Andersen NP, Grøndal AK, Petretto E, Foin N, Davies JE, Mario C, Di Fog Bentzon J, Erik Bøtcher H, Falk E, Krams R, de Silva R. Inducing persistent flow disturbances accelerates atherogenesis and promotes thin cap fibroatheroma development in D374Y-PCSK9 hypercholesterolemic minipigs. *Circulation* 2015;**132**:1003–1012.
  18. Thim T, Hagensen MK, Drouet L, Bal Dit Sollier C, Bonneau M, Granada JF, Nielsen LB, Paaske WP, Bøtcher HE, Falk E, Bøtcher HE, Falk E. Familial hypercholesterolaemic downsized pig with human-like coronary atherosclerosis: a model for preclinical studies. *EuroIntervention* 2010;**6**:261–268.
  19. National Research Council (US) Committee for the Update of the Guide for Care and Use of Laboratory Animals. *Guide for the Care and Use of Laboratory Animals*, 8th ed. Guid. Care Use Lab. Anim. Washington, DC: National Academies Press (US); 2011.
  20. Virmani R, Kolodgie FD, Burke AP, Farb A, Schwartz SM. Lessons from sudden coronary death: a comprehensive morphological classification scheme for atherosclerotic lesions. *Arterioscler Thromb Vasc Biol* 2000;**20**:1262–1275.
  21. Kumar A, Thompson EW, Lefieux A, Molony DS, Davis EL, Chand N, Fournier S, Lee HS, Suh J, Sato K, Ko Y-A, Molloy D, Chandran K, Hosseini H, Gupta S, Milkas A, Gogas B, Chang H-J, Min JK, Fearon WF, Veneziani A, Giddens DP, King SB, Bruyne B, De, Samady H. High coronary shear stress in patients with coronary artery disease predicts myocardial infarction. *J Am Coll Cardiol* 2018;**72**:1926–1935.
  22. Slager CJ, Wentzel JJ, Gijsen FJH, Thury A, Wal AC, van der Schaar JA, Serruys PW. The role of shear stress in the destabilization of vulnerable plaques and related therapeutic implications. *Nat Rev Cardiol* 2005;**2**:456–464.
  23. Koskinas KC, Feldman CL, Chatzizisis YS, Coskun AU, Jonas M, Maynard C, Baker AB, Papafakis MI, Edelman ER, Stone PH. Natural history of experimental coronary atherosclerosis and vascular remodeling in relation to endothelial shear stress: a serial, in vivo intravascular ultrasound study. *Circulation* 2010;**121**:2092–2101.
  24. Koskinas KC, Sukhova GK, Baker AB, Papafakis MI, Chatzizisis YS, Coskun AU, Quillard T, Jonas M, Maynard C, Antoniadis AP, Shi G-P, Libby P, Edelman ER, Feldman CL, Stone PH. Thin-capped atheromata with reduced collagen content in pigs develop in coronary arterial regions exposed to persistently low endothelial shear stress. *Arterioscler Thromb Vasc Biol* 2013;**33**:1494–1504.
  25. Garcia-Garcia HM, Jang I-K, Serruys PW, Kovacic JC, Narula J, Fayad ZA. Imaging plaques to predict and better manage patients with acute coronary events. *Circ Res* 2014;**114**:1904–1917.
  26. Wentzel JJ, Giessen AG, van der Garg S, Schultz C, Mastik F, Gijsen FJH, Serruys PW, van der Steen AFW, Regar E. In vivo 3D distribution of lipid-core plaque in human coronary artery as assessed by fusion of near infrared spectroscopy-intravascular ultrasound and multislice computed tomography scan. *Circ Cardiovasc Imaging* 2010;**3**:e6–e7.
  27. Shishikura D, Sidharta SL, Honda S, Takata K, Kim SW, Andrews J, Montarello N, Delacroix S, Baillie T, Worthley MJ, Psaltis PJ, Nicholls SJ. The relationship between segmental wall shear stress and lipid core plaque derived from near-infrared spectroscopy. *Atherosclerosis* 2018;**275**:68–73.
  28. Millon A, Sigovan M, Bousset L, Mathevet J-L, Louzier V, Paquet C, Geloan A, Provost N, Majd Z, Patsouris D, Serusclat A, Canet-Soulas E. Low WSS induces intimal thickening, while large WSS variation and inflammation induce medial thinning, in an animal model of atherosclerosis. *PLoS One* 2015;**10**:e0141880.
  29. Akyildiz AC, Speelman L, Nieuwstadt HA, Brummelen H, van Virmani R, Lugt A, van der Steen AFW, van der Wentzel JJ, Gijsen F. The effects of plaque morphology and material properties on peak cap stress in human coronary arteries. *Comput Methods Biomech Biomed Engin* 2016;**19**:771–779.
  30. Gao H, Long Q, Graves M, Gillard JH, Li Z-Y. Carotid arterial plaque stress analysis using fluid-structure interactive simulation based on in-vivo magnetic resonance images of four patients. *J Biomech* 2009;**42**:1416–1423.
  31. Li Z-Y, Howarth SPS, Tang T, Gillard JH. How critical is fibrous cap thickness to carotid plaque stability? *Stroke* 2006;**37**:1195–1199.
  32. Laaksonen R, Ekroos K, Sysi-Aho M, Hilvo M, Vihervaara T, Kauhanen D, Suoniemi M, Hurme R, März W, Schramm H, Stojakovic T, Vlachopoulou E, Lokki M-L, Nieminen MS, Klingenberg R, Matter CM, Hornemann T, Jüni P, Rodondi N, Räber L, Windecker S, Gencer B, Pedersen ER, Tell GS, Nygård O, Mach F, Sinisalo J, Lüscher TF. Plasma ceramides predict cardiovascular death in patients with stable coronary artery disease and acute coronary syndromes beyond LDL-cholesterol. *Eur Heart J* 2016;**37**:1967–1976.
  33. Anroedh S, Hilvo M, Akkerhuis KM, Kauhanen D, Koistinen K, Oemrawsingh R, Serruys P, Geuns R-J, van Boersma E, Laaksonen R, Kardys I. Plasma concentrations of molecular lipid species predict long-term clinical outcome in coronary artery disease patients. *J Lipid Res* 2018;**59**:1729–1737.
  34. Schrauwen JTC, Karanasos A, van Ditzhuijzen NS, Aben JP, van der Steen AFW, Wentzel JJ, Gijsen F. The Influence of the accuracy of angiography-based reconstructions on velocity and wall shear stress computations in coronary bifurcations: a phantom study. *PLoS One* 2015;**10**:e0145114.
  35. Wolters B, Slager CJ, Gijsen FJH, Wentzel JJ, Krams R, van der Vosse FN. On the numerical analysis of coronary artery wall shear stress. *Comput Cardiol* 2001;**28**:169–172.

## Translational perspective

Wall shear stress (WSS) plays a key role in coronary atherosclerotic plaque development and destabilization. However, the multidirectionality of WSS is rarely taken into account. In this pre-clinical study, we demonstrated that both plaque initiation and progression were related to low and multidirectional WSS. Therefore, regions exposed to low and/or multidirectional WSS regions throughout disease development, continue to be at risk for further plaque progression. The high predictive values of almost all multidirectional WSS metrics for plaque progression and advanced plaque composition demonstrated the potential of multidirectional WSS as an additional predictive clinical marker for vulnerable disease.